Supplementary Materials

MoS_2 nanosheets vertically grown on $CoSe_2$ hollow nanotube arrays as an efficient catalyst for hydrogen evolution reaction

Liang Yuan[a,b], Yingmeng Zhang[a], Jinhong Chen[a], Yongliang Li[a], Xiangzhong Ren[a], Peixin Zhang[a], Liwei Liu[b], Jinxiang Zhang[c], Lingna Sun[a,*]

[a] College of Chemistry and Environmental Engineering, Shenzhen University, Shenzhen 518060, Guangdong, P. R. China.
[b] College of Physics and Optoelectronic Engineering, Shenzhen University, Shenzhen 518060, Guangdong, P. R. China.
[c] School of Chemistry and Environmental Engineering, Hanshan Normal University, Chaozhou 521041, Guangdong, P. R. China.

[*] Corresponding author. E-mail: sunln@szu.edu.cn.

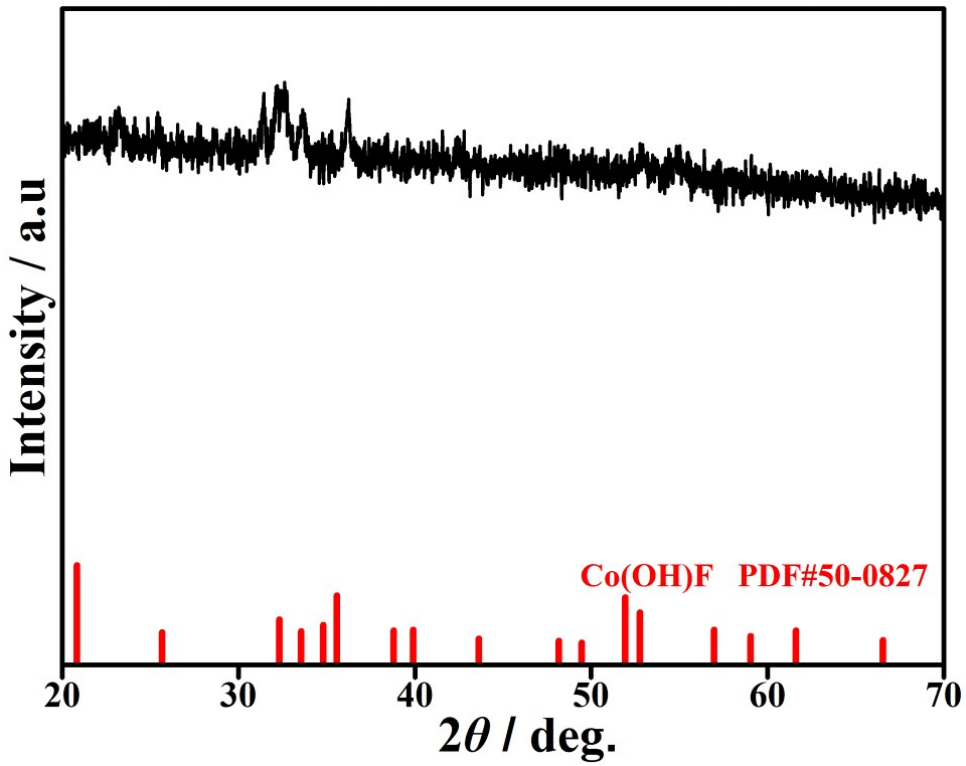

Fig. S1 XRD pattern of Co(OH)F precursor

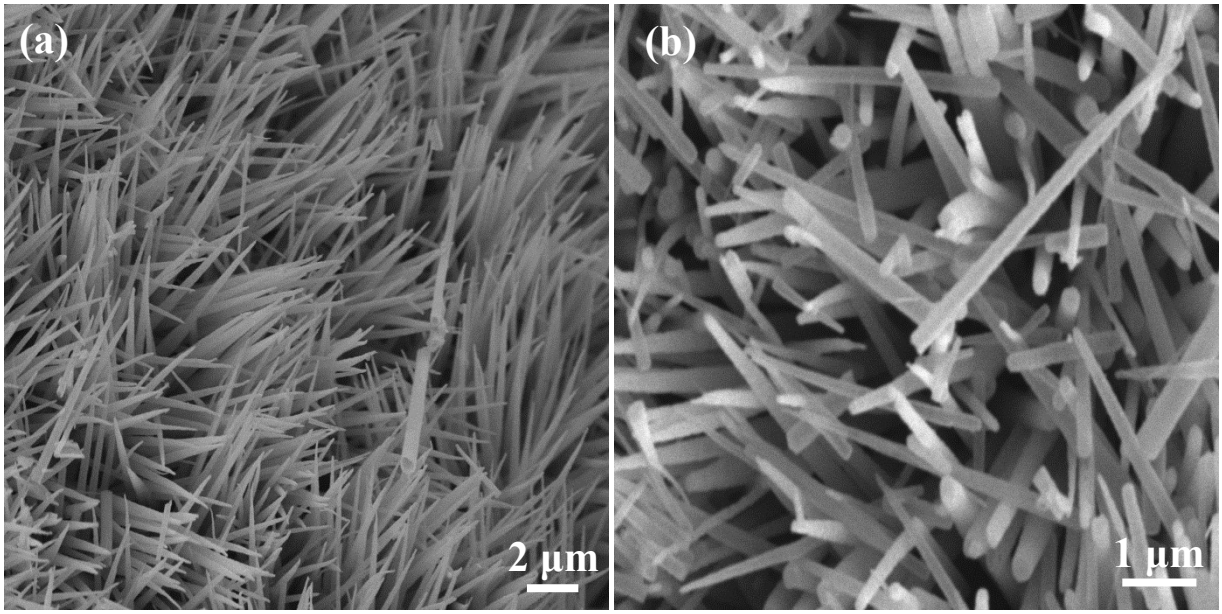

Fig. S2 SEM images of Co(OH)F precursor

(a) × 5000; (b) ×15 k

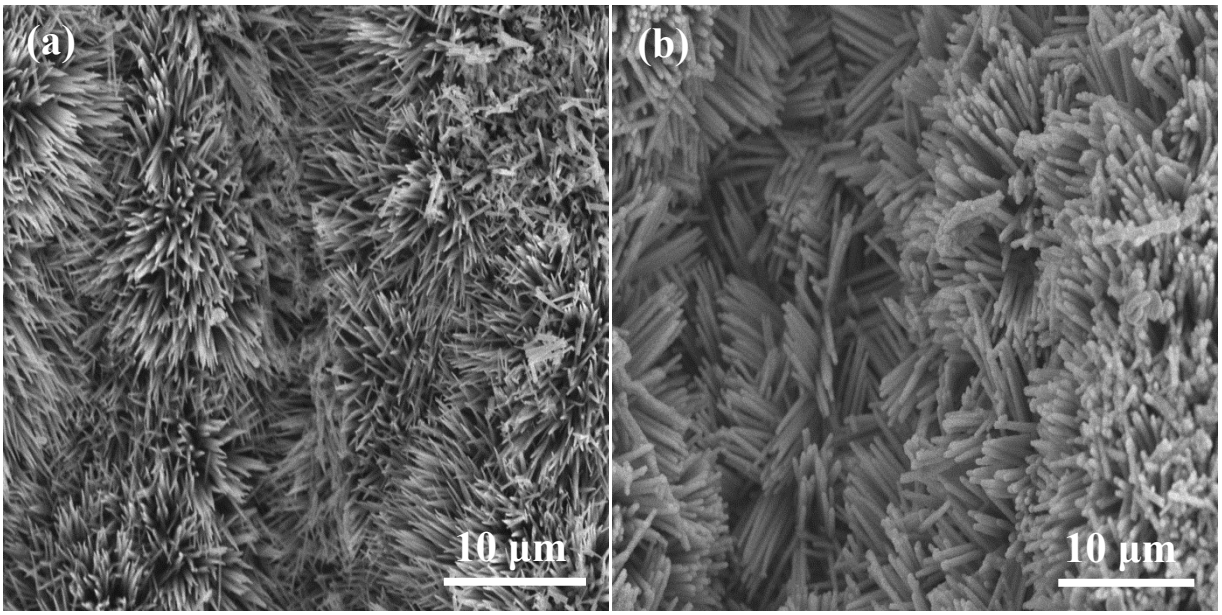

Fig. S3 Low-magnification SEM images of $CoSe_2$-CC and MoS_2@$CoSe_2$-CC

(a) $CoSe_2$-CC; (b) MoS_2@$CoSe_2$-CC

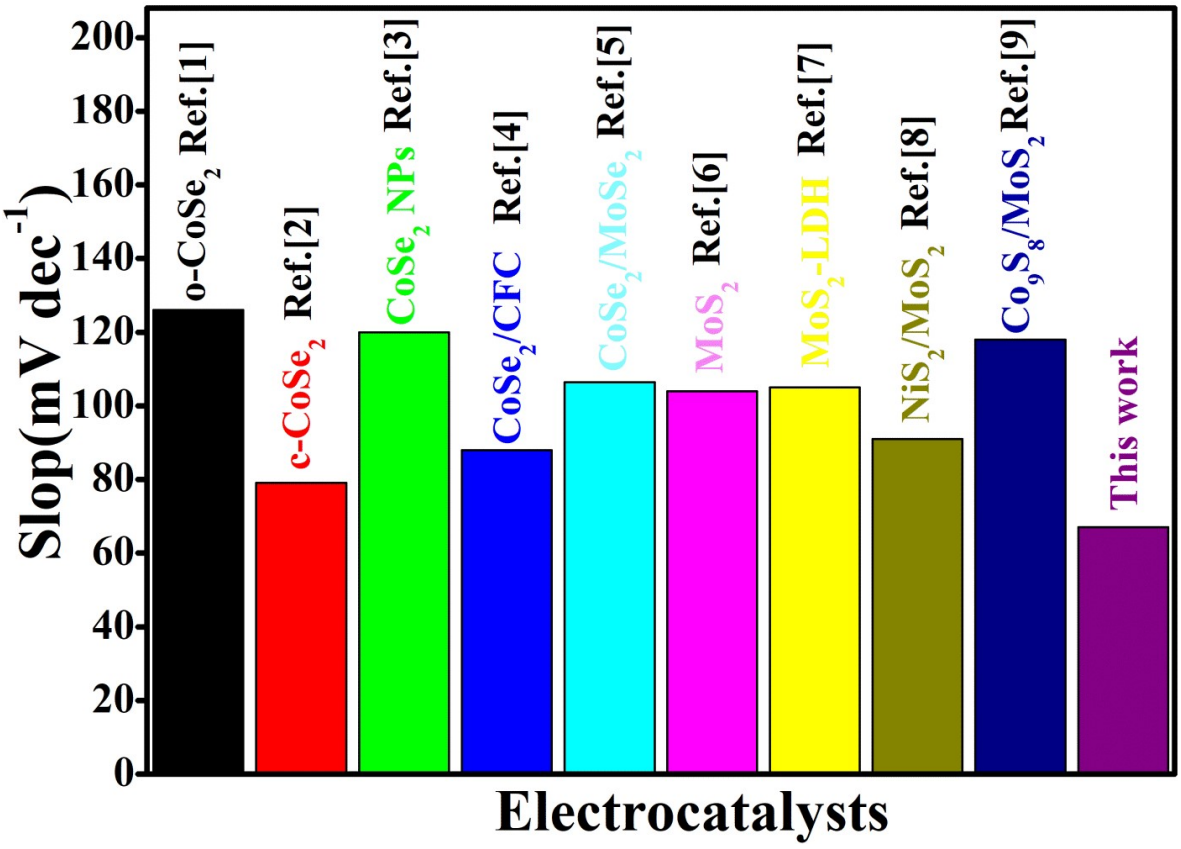

Fig. S4 Comparison of the Tafel slops required to generate a current density of 10 mA cm^{-2} for different MoS_2-base and $CoSe_2$-base catalysts.

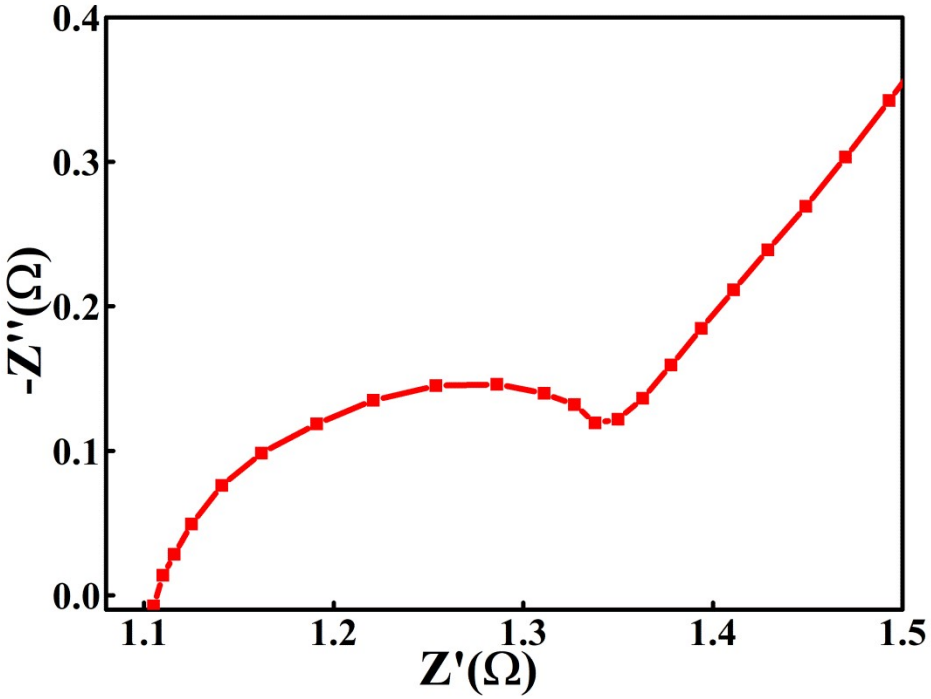

Fig. S5 Nyquist plots of bare $CoSe_2$-CC at high frequency region in 1.0 M KOH

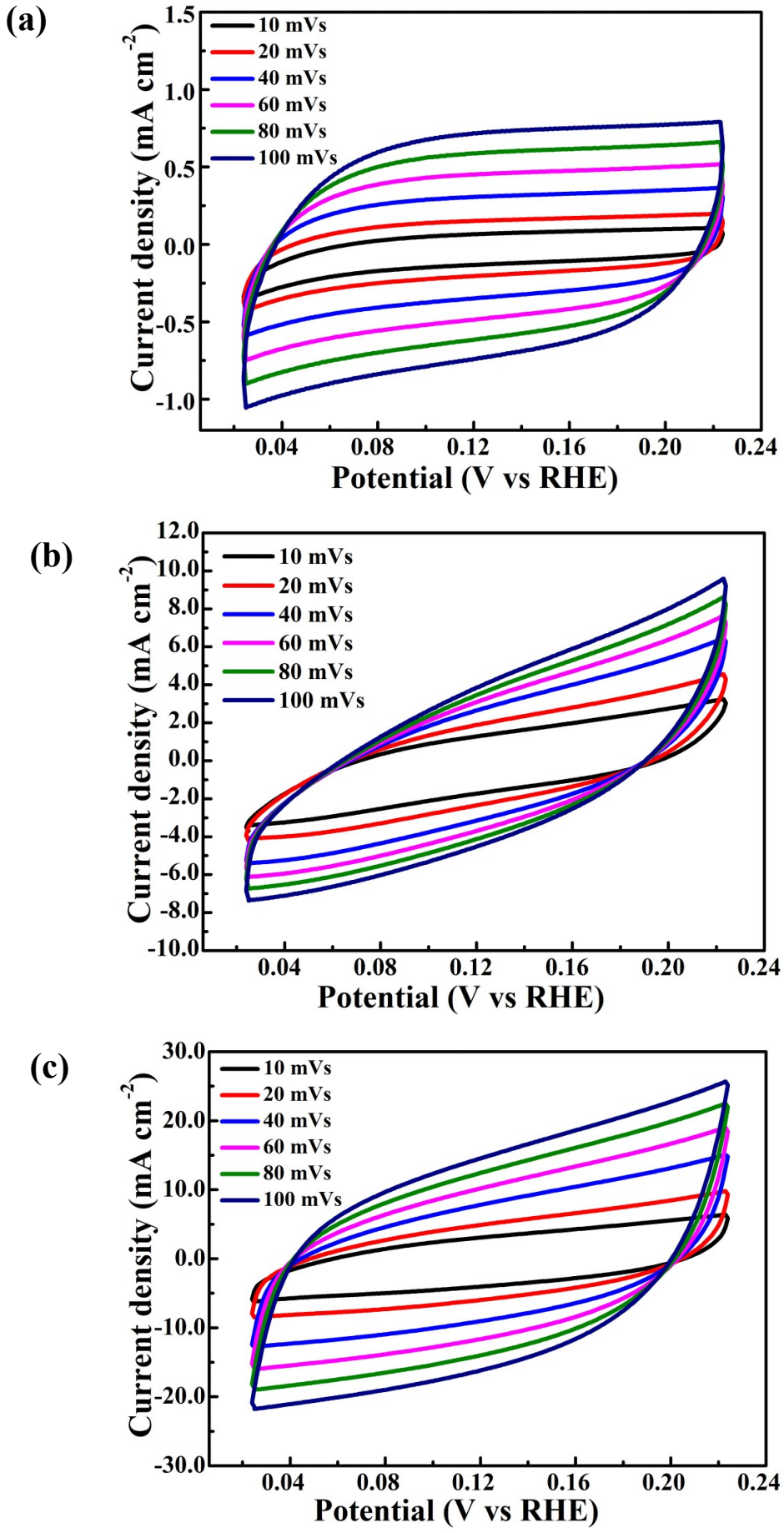

Fig. S6 Typical cyclic voltammogram curves of bare MoS_2-CC, $CoSe_2$-CC and MoS_2@$CoSe_2$-CC hybird in 1.0 M KOH

(a) bare MoS_2-CC; (b) bare $CoSe_2$-CC; (c) MoS_2@$CoSe_2$-CC hybird

S7. Electrochemical Active Surface Area (ECSA) Determination

A fair comparison of TOFs has not yet been carried out due to variations in methods for measuring the active sites in addition to the issues associated with different catalyst structures[10]. Indeed, in most of the cases, ECSA-derived TOFs have afforded a fairer comparison between different electrocatalysts and this method was adopted to calculate TOFs in this work[11-12]. Electrochemical surface area (ECSA) is the ratio of the double layer capacitance to the specific capacitance for a flat surface, so the value of ECSA can be calculated as follows [13]:

$$ECSA = \frac{double\ layer\ capacitance}{specific\ capacitance} \quad (1)$$

The specific capacitance for a flat surface is generally found to fall within the range of 20-60 μF cm^{-2}. Because for many metals and transition metal semiconductors, the double layer capacitance after surface area normalization is comparable in the same electrolyte[14-16]. Therefore, assuming that the specific capacitance of a flat surface is ~40 μF for 1 cm^2 of real surface area, which is a moderate value adopted in this paper and then the ECSA is estimated as:

$$ECSA = \frac{double\ layer\ capacitance\ (mF\ cm^{-2})}{40\ \mu F\ cm^{-2} per\ cm^2_{ECSA}} \quad (2)$$

Assessment of turnover frequency (TOF)

TOF was calculated using the following formula[17]:

$$TOF = \frac{j \times N_A}{2n \times F \times ECSA} \quad (3)$$

where j is the current density at certain overpotential, which can be obtained from HER polarization curves, N_A is the Avogadro's number (6.022×10^{23} molecules/mole), F is the Faraday constant (96485 C mol^{-1}), 2 is the stoichiometric number which represents that two electrons are consumed to form one hydrogen molecule during the electrode HER reaction, n is the number of active sites in a flat 1 cm^2 surface of catalyst samples and ECSA is the electrochemically active surface area of the electrode. The number of surface active sites were estimated to be 1.16×10^{15} cm^{-2} and 4.17×10^{14} cm^{-2} for MoS_2 and $CoSe_2$ based on their lattice constants [18-21], respectively. In addition, the number of surface active sites for MoS_2@$CoSe_2$ hybird can be estimated approximately to be 8.27×10^{14} cm^{-2} by assuming that cobalt selenide molecules are orderly connected with molybdenum sulfide molecules. Similar approach has been used to estimate TOFs for MoS_x@Mo_2C [16] and Ni_9S_8@MoS_2 [18].

Conversion of measured current to H_2 turnover (assuming 100% Faradaic efficiency):

$$TOF = \left(j\frac{mA}{cm^2}\right)\left(\frac{1\ C\cdot s^{-1}}{1000\ mA}\right)\left(\frac{1\ mol\ e^-}{96485\ C}\right)\left(\frac{1\ mol\ H_2}{2\ mol\ e^-}\right)\left(\frac{6.022\times10^{23}\ H_2}{1\ mol\ H_2}\right) = \left(3.12\times10^{15}\frac{H_2\cdot s^{-1}}{cm^2}\right) per\ \frac{mA}{cm^2} \quad (4)$$

So, the number of TOF can be calculated as the following formula:

$$TOF = \frac{3.12\times10^{15}\times|\ j\ |}{The\ number\ of\ surface\ active\ sites} \quad (5)$$

Where j is the current density. Therefore plotted TOFs in the potential range was shown in Fig. S7.

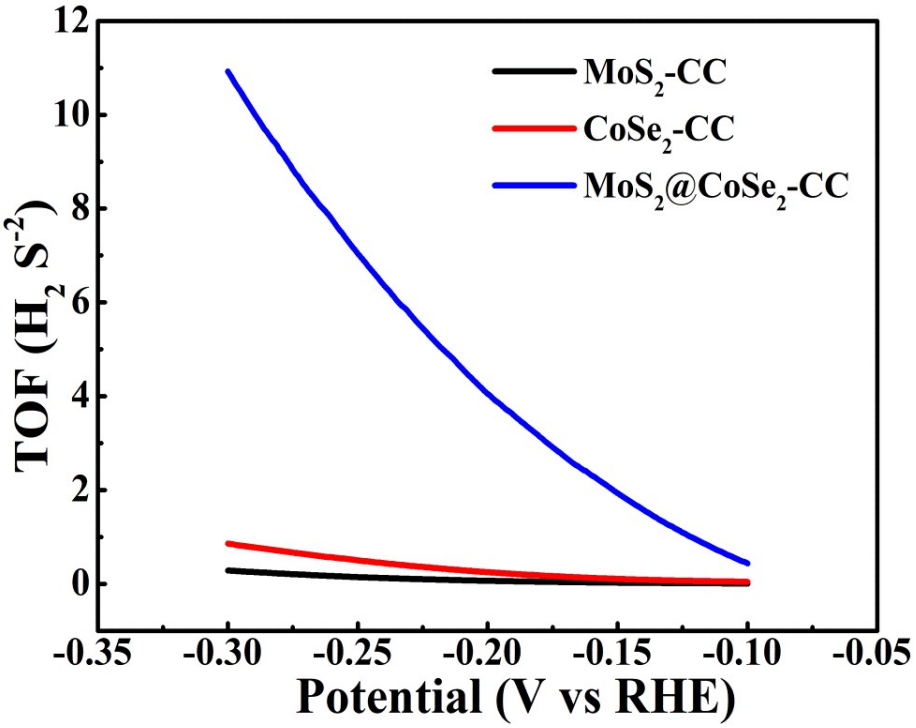

Fig. S7. Turnover frequency (TOF) curves of MoS_2-CC, $CoSe_2$-CC and MoS_2@$CoSe_2$-CC at different potentials.

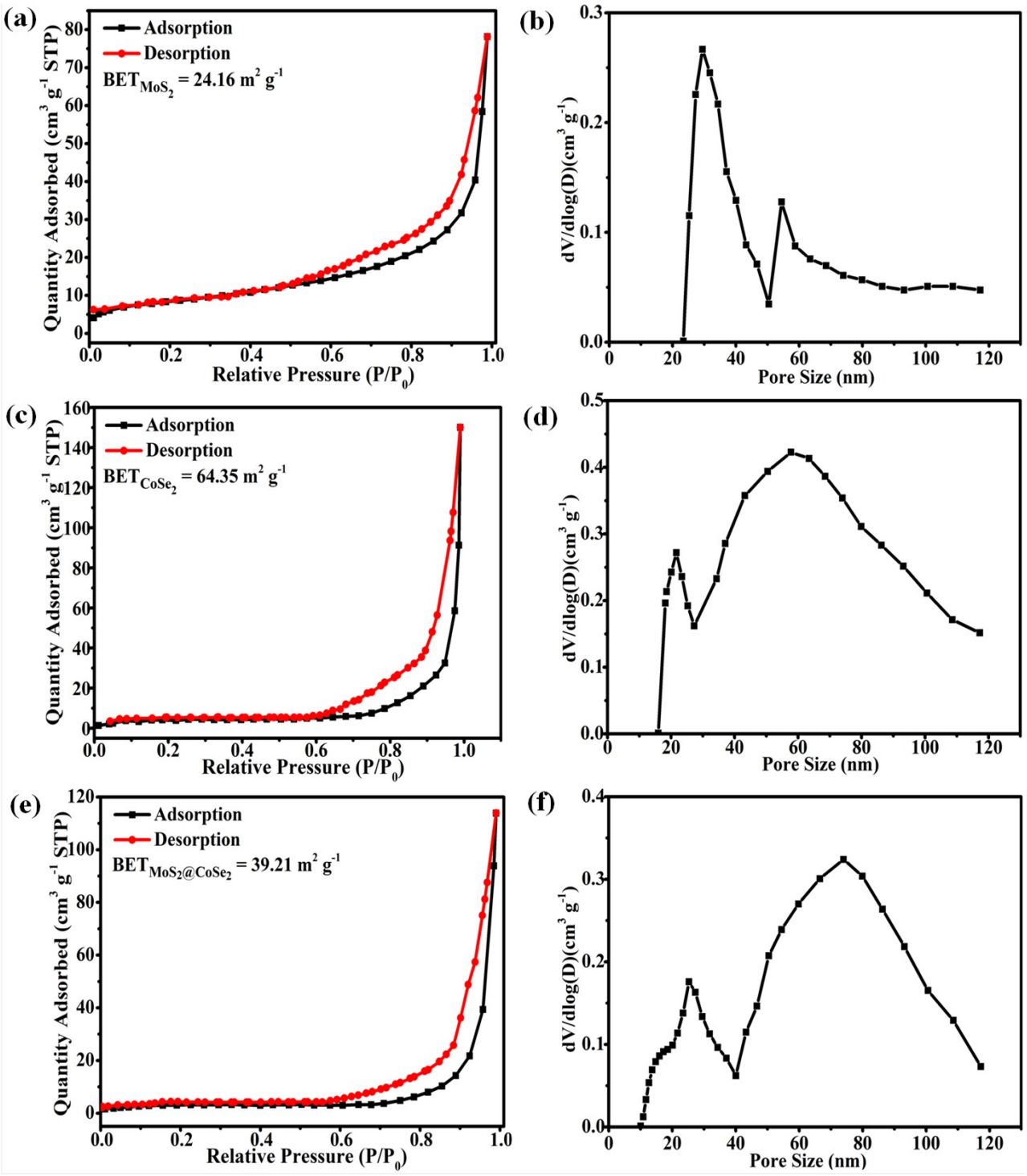

Fig. S8 Nitrogen adsorption-desorption isotherms and size distribution curves of bare MoS_2-CC, $CoSe_2$-CC and MoS_2@$CoSe_2$-CC hybird

(a,b) bare MoS_2-CC; (c,d) bare $CoSe_2$-CC; (e,f) MoS_2@$CoSe_2$-CC hybrid.

Supplementary Table 1. ICP results show the loading of Mo, Co and Se elements in MoS_2@$CoSe_2$-CC catalyst

Element	Co	Mo	Se
Amount (mg L^{-1})	7.149	24.316	21.690

References

[1] P. Chen, K. Xu, S. Tao, T. Zhou, Y. Tong, H. Ding, L. Zhang, W. Chu, C. Wu, Y. Xie. *Adv. Mater*, 2016, **28**, 7527-7532.

[2] H.M. Li, X. Qian, C.L. Zhu, X.C. Jiang, L. Shao, L.X. Hou. *J. Mater. Chem. A*., 2017, **5** 4513–4526.

[3] X.Q. Wang, B.J. Zheng, B.Yu, B. Wang, W.Q. Hou, W.L. Zhang, Y.F. Chen. *J. Mater. Chem. A.,* 2018, **6**, 7842–7850.

[4] Q.C. Dong, Q.Wang, Z.Y. Dai, H.J. Qiu, X.C. Dong. *ACS Appl. Mater. Interfaces*, 2016, **8**, 26902-26907.

[5] X.L. Tang, J.Y. Zhang, B.B Mei, X.M. Zhang, Y.P. Liu, J.X. Wang, W. Li. *Chem. Eng. J*., 2021, **404**, 126529

[6] H. Lin, H. Li, Y. Li, J. Liu, X. Wang, L. Wang. *J. Mater. Chem. A*., 2017, **5**, 25410-25419.

[7] G.Q. Zhao, Y.Lin, K. Rui, Q. Zhou, Y.P. Chen, S.X Dou, W.P. Sun. *Nanoscale*, 2018, **10**, 19074–19081.

[8] X.X. Wang, L. Li, Z. Wang, L. Tan, Z.Y. Wu, Z.L. Liu, S.L. Gai, P.P. Yang. *Electrochim Acta*, 2019, **326**, 134983

[9] T.T. Chen, R. Wang, L.K. Li, Z.J. Li, S.Q. Zang. *J. Energ. Chem*., 2020, **44** , 90–96.

[10] B. Seo, S.H. Joo. *Nano Convergence*, 2017, **4**.

[11] E.J. Popczun, J.R. Mckone, C.G. Read, A.J. Biacchi, A.M. Wiltrout, N.S. Lewis, R.E. Schaak, *J. Am. Chem. Soc*., 2013, **135**, 9267-9270.

[12] B. Seo, D.S. Baek, Y.J. Sa, S.H. Joo, *CrystEngComm*, 2016, **18**, 6083-6089.

[13] Z. Lin, L.F. Shen, X.M. Qu, J.M. Zhang, Y.X. Jiang, S.G. Sun. *Acta Phys. -Chim. Sin*, 2019, **35**, 523–530.

[14] R.Q. Ye, P. del Angel-Vicente, Y.Y. Liu, M.J. Arellano-Jimenez, Z.W. Peng, T. Wang, Y.L. Li, B.I. Yakobson, S.H. Wei, M.J. Yacaman, J.M. Tour. *Adv. Mater*, 2016, **28**, 1427–1432.

[15] J. Kibsgaard, T.F. Jaramillo. *Angewandte Chemie*, 2014, **53**, 14433-14437.

[16] C.Y. Tang, W. Wang, A. Sun, C.K. Qi, D.Z. Zhang, Z.Z. Wu, D.Z. Wang. *ACS Catal*, 2015, **5**, 6956−6963.

[17] Y. Yan, X.M. Ge, Z.L. Liu, J.Y. Wang, J.M. Lee, X. Wang. *Nanoscale*, 2013, **5**, 7768-7771.

[18] X. Xu, W. Zhong, L. Zhang, G. Liu, Y. Du. *J. Colloid Interf. Sci*, 2019, **556**, 24-32.

[19] G. Zhao, P. Li, K. Rui, Y. Chen, S. Dou, W. Sun. *Chem.-Eur. J*, 2018, **24**, 11158-11165.

[20] J.D. Benck, Z. Chen, L.Y. Kuritzky, A.J. Forman, T.F. Jaramillo. *ACS Catal*, 2012, **2**, 1916−1923.

[21] A.I. Carim, F.H. Saadi, M.P. Soriaga, N.S. Lewis. *J. Mater. Chem. A*., 2014, **2**, 13835-13839